Table VIII. Effects of CO Substitution on Bonding in Tetracobalt Clusters[a]

	I[b]	II[c]	VI[d]	VII[e]
$d(Co^{ap}–Co^{ba})$	2.492[a,f]	2.485	2.540	2.472
$d(Co^{ba}–Co^{ba})$	2.492[f]	2.457	2.457	2.447
$d(Co^{ba}–CO^{br})$	2.043	1.948	1.933	1.912
$d(Co^{ap}–CO^{ap})$	1.834[g]		1.793	
$d(Co^{ba}–CO^{t})$	1.834[g]	1.783	1.752	1.740
ν_{CO}, CO^{br}	1868 (pentane)	1829 (hexane)	1780 (CH_2Cl_2)	1740 (CH_2Cl_2)

[a] All distance in Å; ν_{CO} in cm^{-1}. [b] I = $Co_4(CO)_{12}$, from ref 47. [c] II = (η-C_6H_6)$Co_4(CO)_9$, from ref 48. [d] VI = $Co_4(CO)_9$(tripod), from ref 50. [e] VII = (η-MeC_6H_5)$Co_4(CO)_6$(tripod), from ref 39. [f] Average values taken over all Co-Co distances because of disorder in crystal. [g] Average values taken over all Co-to-terminal CO distances because of disorder in crystal.

kinetic pathways to cluster degradation, rearrangement, and substitution. Cyclic voltammetric studies of $Co_4(CO)_{12}$ in THF showed rapid cluster decomposition; no such fragmentation was observed in our studies of tripod-substituted tetracobalt clusters in either THF or CH_2Cl_2. One interpretation of the different electrochemical stabilities of I and tripod derivatives is that the chelating tripod ligand in analogues of III inhibits irreversible metal–metal bond cleavage following electron transfer. Enhanced reversibility in the electrochemical behavior of Co_4 dppm-substituted clusters has also been attributed to bridging ligand effects.[32a] Tripod ligand stabilization of reduced clusters by charge delocalization may be ruled out since ground-state calculations on the clusters $Co_4(CO)_9[(PH_2)_3CH]$ and (η-C_6H_6)Co_4-$[(PH_2)_3CH]$ show little $(PH_2)_3CH$ character in the frontier orbitals (Table III).

Bridging of metal–metal bonds with multidentate ligands does not appear to be the sole reason for increased electrochemical stability, since the toluene-capped cluster V is also reduced reversibly. Crystal structure determinations[39,47,48,50] have shown that coordination of an apical arene to a tetracobalt cluster results in the shortening of the apical–basal metal–metal bond,[50] Table VIII. These stronger apical–basal interactions help rationalize the greater electrochemical stability of V and VII compared to I. As mentioned earlier (η-arene)M fragments are better suited to metal–metal bonding than the isolobal $M(CO)_3$ fragment.[56] Donor ligands also cause stronger (μ-CO)Co_2 interactions through increased metal-to-Co back-bonding, thereby hindering metal–metal bond fragmentation. Stronger metal to bridging CO bonding is suggested by the lower stretching frequency, ν_{CO}, observed in the substituted clusters (Table VIII). The metal–CO distance for bridging carbonyls also decreases with substitution, reflecting a stronger bonding interaction. A similar decrease is seen in terminal carbonyl–metal distances.

Acknowledgment. We thank Dr. J. G. Gaudiello for valuable advice about the electrochemical measurements. This material is based on work supported by the National Science Foundation (Grants DMR82-14966 to D.E.E. and CHE84-02168 to W.C.T.). W.C.T. thanks the Sloan Foundation for a research fellowship.

Pairwise Exchange of Carbon Monoxide in Manganese–Rhenium Decacarbonyl

Steven P. Schmidt,[1a] Fred Basolo,*[1a] Craig M. Jensen,[1b] and William C. Trogler*[1b]

Contribution from the Department of Chemistry, Northwestern University, Evanston, Illinois 60201, and the Department of Chemistry, D-006, University of California at San Diego, La Jolla, California 92093. *Received September 30, 1985*

Abstract: Manganese–rhenium decacarbonyl, selectively enriched on the rhenium atom, is prepared by the rapid reaction between $KMn(CO)_5$ and $Re(^{13}CO)_5(O_3SCF_3)$ that was isotopically enriched to 46%. At temperatures between 65 and 85 °C migration of the label to the Mn atom occurs according to a first-order rate law (k(65 °C) = 0.47 ± 0.09 × 10^{-4} s^{-1}). The reaction is monitored by low-temperature ^{13}C NMR spectroscopy: Mn–C_{ax} δ 215.4; Mn–C_{eq} δ 220.4; Re–C_{ax} δ 179.6; Re–C_{eq} δ 190.5. Activation parameters (ΔH^{*} = 12.7 ± 1.4 kcal/mol, ΔS^{*} = −41 ± 6 cal/(mol K)), in particular the large negative entropy, are consistent with a pairwise CO exchange mechanism.

Dimanganese, dirhenium, and manganese–rhenium decacarbonyl are prototypical compounds for examining the mechanisms of reaction of metal–metal bonded carbonyls. Carbonyl substitution reactions generally proceed by CO dissociation,[2-5] however, metal-metal bond homolysis has been observed[6] for certain phosphine-substituted manganese dimers. Oxidation reactions of the metal–metal bond take place by both inner- and outer-sphere mechanisms.[7] Irradiation of the parent carbonyls with ultraviolet light leads to metal–metal bond homolysis and the production of 17-electron radical intermediates.[8] Carbonyl-bridged intermediates have been proposed[5] to explain anomalous product distributions in substitution reactions of $MnRe(CO)_{10}$ as well as for photochemical reactions of metal cluster compounds in which the metal–metal bond may be broken.[9] Irradiation of

---

(1) (a) Northwestern University. (b) University of California at San Diego.

(2) Basolo, F.; Wawersik, H. *Inorg. Chim. Acta* **1969**, *3*, 113–120.

(3) Schmidt, S. P.; Trogler, W. C.; Basolo, F. *Inorg. Chem.* **1982**, *21*, 1698–1699.

(4) Muetterties, E. L.; Burch, R. R.; Stolzenberg, A. M. *Annu. Rev. Phys. Chem.* **1982**, *33*, 89–118.

(5) Sonnenberger, D.; Atwood, J. D. *J. Am. Chem. Soc.* **1980**, *102*, 3484–3489.

(6) Poë, A.; Sekhar, C. V. *J. Am. Chem. Soc.* **1985**, *107*, 4874–4883.

(7) Schmidt, S. P.; Trogler, W. C.; Basolo, F. *J. Am. Chem. Soc.* **1984**, *106*, 1308–1313. Schmidt, S. P.; Trogler, W. C.; Basolo, F., to be submitted.

(8) Wrighton, M. S.; Ginley, D. S. *J. Am. Chem. Soc.* **1975**, *97*, 2065–2072. Kidd, D. R.; Brown, T. L. *J. Am. Chem. Soc.* **1978**, *100*, 4095–4103.

(9) Desrosiers, M. F.; Ford, P. C. *Organometallics* **1982**, *1*, 1715–1716. Malito, J.; Markiewitz, S.; Poë, A. *Inorg. Chem.* **1982**, *21*, 4335–4337. Desrosiers, M. F.; Wink, D. A.; Ford, P. C. *Inorg. Chem.* **1985**, *24*, 1–2.

0002-7863/86/1508-1894$01.50/0

$Mn_2(CO)_{10}$ in a methylcyclohexane glass at 77 K yields[12] CO and $Mn_2(CO)_9$ that contains a bridging CO group. Mechanistic proof of CO-bridged intermediates for complexes that contain only terminal CO groups remains difficult to probe. Furthermore, the mechanism of carbonyl migration in unbridged trinuclear complexes is the subject of some controversy[10,11] and has been proposed to involve both type A and B intermediates. Despite spectroscopic evidence in support of both intermediates,[11] the mechanism of this process remains a matter of speculation. Herein we report the synthesis of $MnRe(CO)_{10}$ that is specifically labeled with ^{13}CO on Re. Evidence for pairwise CO exchange and for a high barrier to migration of CO across the nonbridged Mn–Re single bond has been obtained.

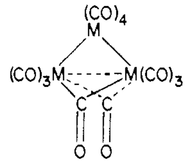

A

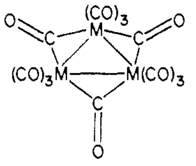

B

Experimental Section

Materials. Chloroform and dichloromethane were distilled from P_2O_5 Tetrahydrofuran was dried over sodium benzophenone ketyl and distilled before use. Acetonitrile (Burdick and Jackson, 0.01% H_2O) was purified by three successive distillations under nitrogen, the first from CaH_2 and those following from P_2O_5 (~ 5 g/L). Iodine (Mallinckrodt), and silver trifluoromethanesulfonate (Aldrich) were used as received. Isotopically labeled ^{13}CO (99.9% molecular purity, 93.1% isotopic purity) was obtained from Koch Isotopes and stored in a gas bulb over activated silica gel (6–16 mesh, Baker).

Preparations. All manipulations were carried out under an atmosphere of prepurified nitrogen with use of standard Schlenk techniques. Solids were handled and stored in a Vacuum Atmospheres glovebox equipped with an HE-493 dri train. A high-vacuum line was used to transfer ^{13}CO and to degas solutions. The compounds $Re(CO)_5Cl$[13] and $KMn(CO)_5$[14] were prepared by known[13,14] methods.

IR spectra were recorded with a Perkin-Elmer 283 or a Nicolet 7199 FT-IR spectrometer using variable path length (0.1–0.5 mm) CaF_2 or KBr cells and a 1 dm KBr gas cell. Mass spectra were obtained with a HP 5985A GC/MS or at the U.C. Riverside mass spectral facility. Isotopic compositions were determined with the use of the MASPAN program[15] and a VAX 11/750 computer.

$Re(^{13}CO)_5Cl$. A 0.230-g sample of $Re(CO)_5Cl$ (0.64 mmol) was dissolved in 25 mL of $CHCl_3$ contained in a 100-mL flask adapted for use on a high vacuum line. The entire flask was evacuated and cooled to 77 K before introducing 290 mm of ^{13}CO (a ratio $^{13}CO/^{12}CO$ of ~1.4). The solution was stirred vigorously and placed in a constant temperature bath at 40.0 °C for 5 h. This temperature maximized CO exchange and minimized formation of the chloro-bridged dimer. The IR spectrum of the reaction solution showed 9 carbonyl bands as expected,[16] the most prominent at 2148 (w), 2138 (w), 2127 (s), and 1944 (m) cm^{-1}. ^{13}C NMR ($CDCl_3$, 25 °C) δ 178.5 (ax), 176.5 (eq). The compound was left in the flask after removal of $CHCl_3$ under reduced pressure, assuring a one-to-one stoichiometry in the ensuing metathesis reactions.

$Re(^{13}CO)_5(O_3SCF_3)$. The synthesis[17] of the unlabeled compound was modified. To a solution of $Re(^{13}CO)_5Cl$ (0.64 mmol) dissolved in 20 mL of CH_2Cl_2 was added 0.250 g of $AgCF_3SO_3$ (0.97 mmol) under a stream of nitrogen. After the mixture was stirred for 4 h at room temperature an IR spectrum of the solution shows 9 carbonyl bands for $Re(^{13}CO)_5(O_3SCF_3)$, all shifted to higher frequency from the chloro derivative. In addition, the IR spectrum showed ν_{SO} 1006 (s), 1172 (m), and 1342 (m) cm^{-1}. After removal of CH_2Cl_2 under reduced pressure the compound was used in the following synthesis.

$(OC)_5MnRe(^{13}CO)_5$. The $Re(^{13}CO)_5X$ (X = Cl or O_3SCF_3) prepared previously (0.64 mmol) was dissolved in 15 mL of THF in a 50-mL Schlenk flask wrapped in foil. To an addition funnel containing 15 mL of THF, $KMn(CO)_5$ (0.154 g, 0.66 mmol) was added by ampule under a stream of N_2. After the funnel was shaken a clear, green solution results. The exact volume of $KMn(CO)_5$ solution (14.5 mL, 0.64 mmol) necessary was added drop by drop over a 20-min period. The solution initially turned bright yellow and, after addition of all the $KMn(CO)_5$, became bright orange. The reaction was monitored by IR spectroscopy to verify total disappearance of both monomeric carbonyl fragments. Three different procedures I–III were employed for the reaction.

Compound I. With use of $Re(^{13}CO)_5Cl$, the reaction mixture was stirred in the dark for 25 h and then equipped with a condenser and refluxed (66 °C) for 2 h until IR absorptions of $KMn(CO)_5$ and $Re(^{13}CO)_5Cl$ disappear. Evaporation of solvent at room temperature afforded a yellow-orange solid. Sublimation of the residue at 80 °C and 0.1 mm Hg yielded lemon-yellow crystals (34%, 0.096 g, 0.18 mmol). As seen later this synthesis yields product with scrambled label.

Compound II. Again, with $Re(^{13}CO)_5Cl$ the reaction mixture was stirred in the dark at room temperature for 111 h. The THF was removed at room temperature under vacuum. Hexane (25 mL distilled from Na) was added and the solution stirred, removed by syringe, and filtered through a medium frit. This extraction process was repeated with an additional 10 mL of hexane. Removal of solvent under reduced pressure afforded lemon-yellow crystals of $MnRe(CO)_{10}$, compound II, in 45% yield.

Compound III. The metathesis reaction was complete within 15 min after addition of $KMn(CO)_5$ to $Re(^{13}CO)_5(O_3SCF_3)$ in THF. After removal of solvent, the residue was extracted by vigorous stirring ($^1/_2$ h) with 30 mL of hexane. The cloudy, yellow solution was filtered through a fine frit and labeled $MnRe(CO)_{10}$, compound III, formed as lemon-yellow crystals in 86% yield after removal of hexane under vacuum.

Reaction between Labeled $MnRe(CO)_{10}$ and I_2. A sample of $MnRe(CO)_{10}$, labeled with ^{13}CO by any of the methods I–III (0.017 g, 0.03 mmol), was dissolved in 10 mL of CH_3CN. Iodine (0.041 g, 0.161 mmol) was added under a nitrogen stream and the resulting red-brown solution was stirred for 5 min at room temperature. An IR spectrum of the solution confirmed the production of $Mn(CO)_5I$ and $[Re(CO)_5(NCCH_3)]^+$. The solvent and the excess I_2 were removed under reduced pressure. Sublimation at 40 °C and 0.1 mm Hg affords orange crystals of $Mn(CO)_5I$.

Kinetic Studies. Typically, 5-mm NMR tubes were charged with 0.010 g (0.019 mmol) of 24% ^{13}CO enriched $(CO)_5MnRe(CO)_5$, III. The tubes were placed under nitrogen and, following addition of 0.3 mL of toluene-d_8, sealed under vacuum. After being loaded, the NMR tubes were placed in a Brinkman RM7 constant temperature (±0.05 °C) bath. At the end of the prescribed heating period the samples were stored briefly at −15 °C pending ^{13}C NMR analysis. When procedures were developed that gave consistent (±10%) rate constants at a single temperature, a single series of samples were prepared and used for the kinetic determinations. The ^{13}C NMR spectra for each data point were obtained (50.31 MHz) at −65 °C with a Nicolet 200 spectrometer equipped with a variable-temperature controller. The quaternary carbon resonance of toluene-d_8 solvent was used as an internal standard for all integrations. All integrations were performed for spectra recorded at the same temperature and the same set of instrumental parameters (pulse delay = 1 s, 14 μs pulse, 508 ms acquisition time). Because the integrated intensities of Mn and Re carbonyl resonances were 1:1 in a statistically labeled sample of $MnRe(CO)_{10}$ there is no correction necessary for differing relaxation times. Spectra were integrated and first-order plots of ln ($I_\infty - I_t$) for the equatorial CO resonance on Re were linear for 2 half-lives. The I_∞ value was verified to be 50% of the initial amount of ^{13}CO label by ^{13}C NMR analysis. Thereafter this value was assumed in all kinetic analyses. Errors were determined by a linear least-squares analysis program with the use of an IBM 9000 computer system. Because of the low intensity of the axial carbonyl resonance on Re only approximate rate

---

(10) (a) Forster, A.; Johnson, B. F. G.; Lewis, J.; Matheson, T.; Robinson, B. H.; Jackson, W. G. *J. Chem. Soc., Chem. Commun.* **1974**, 1042. (b) Aime, S.; Gambino, L.; Milone, L.; Sappa, E.; Rosenberg, E. *Inorg. Chim. Acta* **1975**, *15*, 53–57. (c) Cotton, F. A.; Jamerson, J. D. *J. Am. Chem. Soc.* **1976**, *98*, 5396–5399.

(11) (a) Johnson, B. F. G.; Lewis, J.; Reichert, B. E.; Schorpp, K. T. *J. Chem. Soc., Dalton Trans.* **1976**, 1403–1404. (b) Tachikawa, M.; Richter, S. I.; Shapley, J. R. *J. Organomet. Chem.* **1977**, *128*, C9–C14. (c) Koridze, A. A.; Kizas, O. A.; Astakhova, N. M.; Petroviskii, P. V.; Grishin, Y. K. *J. Chem. Soc., Chem. Commun.* **1981**, 853–854. (d) Deeming, A. J.; Donovan-Mtunzi, S.; Kabir, S. *J. Organomet. Chem.* **1985**, *281*, C43–C46. (e) Cotton, F. A.; Hanson, B. E.; Jamerson, J. D. *J. Am. Chem. Soc.* **1977**, *99*, 6588–6594. (f) Cotton, F. A.; Hanson, B. E. *Inorg. Chem.* **1977**, *16*, 2820–2822.

(12) Hepp, A. F.; Wrighton, M. S. *J. Am. Chem. Soc.* **1983**, *105*, 5934–5935.

(13) Schmidt, S. P.; Trogler, W. C.; Basolo, F. *Inorg. Synth.* **1985**, *23*, 41–46.

(14) Gladysz, J. A.; Williams, G. M.; Tam, W.; Johnson, D. L.; Parker, D. W.; Selover, J. C. *Inorg. Chem.* **1979**, *18*, 553–558.

(15) Knox, S. A. R.; Koepke, J. W.; Andrews, M. A.; Kaesz, H. D. *J. Am. Chem. Soc.* **1975**, *97*, 3942–3947.

(16) Kaesz, H. D.; Bau, R.; Hendrickson, D.; Smith, J. M. *J. Am. Chem. Soc.* **1967**, *89*, 2844–2851.

(17) Schmidt, S. P.; Nitschke, J.; Trogler, W. C. *Inorg. Synth.*, in press.

Table I. Carbonyl Stretching Frequencies (ν_{CO}, cm^{-1}) for $MnRe(CO)_{10}$ and ^{13}CO-Substituted Species

MnRe-$(CO)_{10}$^{a}	^{13}CO Substituted Species^b		$(O^{13}C)_5MnRe$-$(^{13}CO)_5$^{c} (II)
2124.5	axial ^{13}CO–Mn^b	1946.0	2123.9
2054.5	equatorial ^{13}CO–Mn	1995.5	2117.7
1991.0		1991.0	2054.1
1978.0		1946.0	2050.7
2039.0	axial ^{13}CO–Re	1945.0	2046.3
2007.0	equatorial ^{13}CO–Re	2118.0	2034.2
2017.5		2033.0	2031.2
1976.0		2000.5	2017.8
		1992.0	2003.1
			1999.7
			1997.2
			1994.3
			1986.8
			1979.2
			1969.7
			1964.7
			1956.6
			1945.8

^{a} Flitcroft, N.; Huggins, D. K.; Kaesz, H. D. *Inorg. Chem.* **1964**, *3*, 1123–1130. ^{b} Reference 19. ^{c} In hexane solution at 0.25-cm^{-1} resolution.

constants for axial exchange could be obtained. Activation parameters were calculated from a linear least-squares fit of temperature-dependent rate data to the Eyring equation.

Results and Discussion

Synthesis and Characterization of Labeled Complexes. Three procedures were used in an attempt to prepare selectively ^{13}CO-enriched $MnRe(CO)_{10}$, eq 1–3. The $Re(^{13}CO)_5Cl$ was enriched

$$KMn(CO)_5 + Re(^{13}CO)_5Cl \xrightarrow[\text{2 h (66 °C)} \atop \text{THF}]{\text{24 h (20 °C)}} I + KCl \quad (1)$$

$$KMn(CO)_5 + Re(^{13}CO)_5Cl \xrightarrow[\text{THF}]{\text{111 h (20 °C)}} II + KCl \quad (2)$$

$$KMn(CO)_5 + Re(^{13}CO)_5(O_3SCF_3) \xrightarrow{\text{15 min (20) °C)}} \underset{\text{III}}{(OC)_5Mn\text{–}Re(^{13}CO)_5} \quad (3)$$

to 46% (deconvolution of the parent mass multiplet with the MASPAN program[15]) by the slow exchange reaction between ^{13}CO and $Re(CO)_5Cl$ as described in the Experimental Section. These reactions show that triflate $(O_3SCF_3^-)$ is a superior leaving group as compared to chloride for attack by metal anions to yield cluster compounds. The exceptional lability of triflate toward substitution by neutral ligands has already been established.[18]

Analysis of products I–III by FTIR spectroscopy (Table I) was not informative. All three complexes exhibited similar IR spectra and the 18 absorptions found for II are provided in Table I. Spectra of complex III (Figure 1) differ slightly from those of I and II as the IR peaks at 2051.8 and 1943.0 cm^{-1} shift and become more intense. The procedure used to synthesize II was *analogous* to one claimed[19] to produce $MnRe(CO)_{10}$ with ^{13}CO label only on Re. Because of the inconclusive IR data we sought an alternative spectroscopic probe.

The ^{13}C NMR spectra of $Mn_2(CO)_{10}$ and $Re_2(CO)_{10}$ have been reported:[20] $Mn_2(CO)_{10}$–(CH_3Cl, 25 °C) δ 223.1 (CO axial), δ 212.9 (CO equatorial); $Re_2(CO)_{10}$–(THF, −60 °C); δ 183.7 (CO axial), δ 192.7 (CO equatorial). At room temperature complexes I–III all exhibit ^{13}C resonances (in toluene-d_8) at δ 190.5 and 179.6 (relative to the carbon of toluene at 139.4 ppm) in a 4:1 intensity ratio attributable to equatorial and axial carbonyl resonances on Re. Because thermal decoupling[21] sometimes allows one to observe NMR spectra of nuclei bound to quadrupolar Mn, spectra were also obtained at −72 °C. Two additional signals appear at δ220.4 and 215.4 in the spectra of I and II but not III. The 4:1 intensity ratio dictates their assignment to equatorial and axial carbonyl resonances bound to manganese. The 1:1 ratio of integrated intensities for carbonyl resonances of Mn and Re suggest that compounds I and II contain ^{13}CO distributed equally over Mn and Re, whereas compound III is labeled predominantly on Re. Deconvolution[15] of the parent ion multiplet of III (in the mass spectrum) yields a value of 24% ^{13}CO enrichment. Having previously found 46% enrichment for $Re(^{13}CO)_5Cl$ this shows complete retention of label in the synthesis of the dimer.

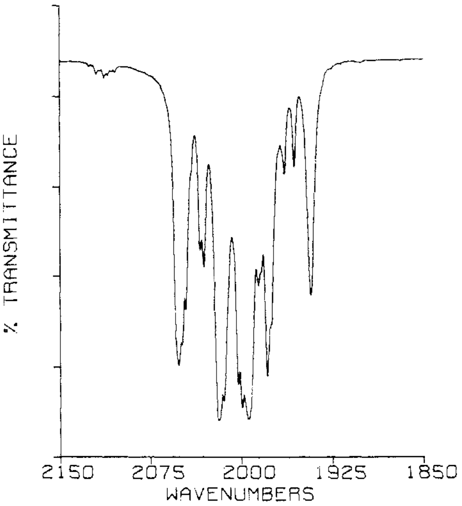

Figure 1. Fourier transform IR spectrum of $(OC)_5MnRe(^{13}CO)_5$ (III) in hexane solvent.

Analysis of products from the iodine cleavage reaction, eq 4, further supports the isotopic distribution of ^{13}CO on Re in III. The IR spectrum of $Mn(CO)_5I$ obtained from the reaction of III

$$MnRe(CO)_{10} + 2I_2 \xrightarrow[CH_3CN]{} Mn(CO)_5I + [Re(CO)_5(NCCH_3)]I_3 \quad (4)$$

showed no difference from the spectrum of an authentic sample[16] of unlabeled $Mn(CO)_5I$. For compound I and II the $Mn(CO)_5I$ produced showed extra IR absorptions at 2119.2 (w), 2110.1 (w), 2067.1 (w), 2015.9 (m), and 1960.0 cm^{-1} (w) identical with those reported [16] to appear when $Mn(CO)_5I$ is allowed to exchange with ^{13}CO. Deconvolution[15] of the parent ion multiplet in the mass spectra of $Mn(CO)_5I$ obtained from eq 4 for I and III shows 17% and 1.5% ^{13}CO incorporation, respectively.

Kinetics of CO Exchange. The preceding results suggest that CO exchange occurs intramolecularly during the formation of I and II. Intermolecular exchange (eq 5) was followed by FTIR spectroscopy for the reaction between unlabeled $MnRe(CO)_{10}$ and

$$MnRe(^{12}CO)_{10} \xrightarrow[\text{120 °C, decalin}]{^{13}CO} MnRe(^{12}CO)_{10-x}(^{13}CO)_x + x(^{12}CO) \quad (5)$$

^{13}CO in decalin. Absorptions at 2032.8 (w), 1997.5 (m), 1967.3 (mw), and 1943.3 (mw) cm^{-1} appear during the exchange reaction. Monitoring the rate of disappearance of the parent absorption at 2053.9 cm^{-1} yields an approximate first-order rate constant of 1.6×10^{-5} s^{-1} at 120 °C. A ^{13}C NMR of the exchanged product was obtained by removing the decalin solvent and dissolving the labeled $MnRe(CO)_{10}$ in $CDCl_3$. The spectrum at −30 °C showed that ^{13}CO is found on both Mn and Re. Since the rate of in-

---

(18) Nitschke, J.; Schmidt, S. P.; Trogler, W. C. *Inorg. Chem.* **1985**, *24*, 1972–1978.

(19) Wozniak, W. T.; Evans, G. O., II; Sheline, R. K. *J. Inorg. Nucl. Chem.* **1975**, *37*, 105–108.

(20) Todd, L. J.; Wilkinson, J. R. *J. Organomet. Chem.* **1974**, *77*, 1–27.

(21) Todd, L. J.; Wilkinson, J. R. *J. Organomet. Chem.* **1974**, *80*, C31–C34.

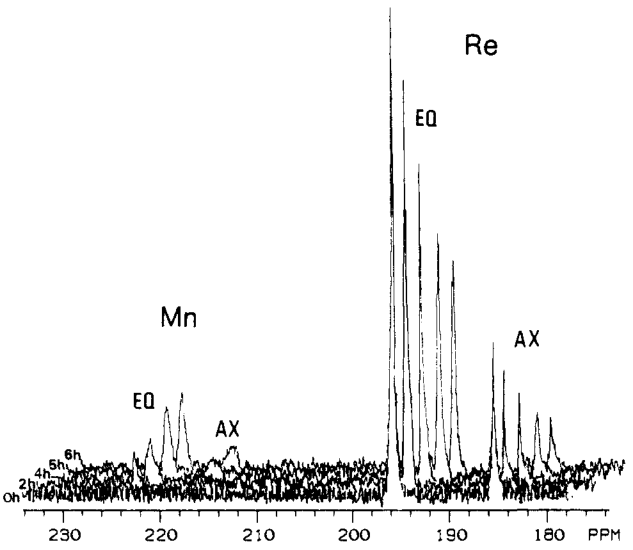

Figure 2. Successive ^{13}C NMR spectra in toluene-d_8 showing the transfer of ^{13}CO label from rhenium to manganese at 75 °C. At equilibrium the integrated intensities of the Mn and Re carbonyls were 1:1. Times given are the hours the solution of III was heated at 75 °C before recording the spectrum at −65 °C.

Table II. Rate Constants and Activation Parameters[a] for Intramolecular Equatorial CO Exchange in $MnRe(CO)_{10}$

temp. °C	$[MnRe(CO)_{10}]$, M	$k_{obsd} \times 10^4$, s^{-1}
65.0	0.064	0.47 ± 0.09
75.0	0.064	0.80 ± 0.15
85.0	0.064	1.43 ± 0.09
85.0	0.032	1.46 ± 0.03

$\Delta H^{\ddagger\,a} = 12.7 \pm 1.4$ kcal/mol
$\Delta S^{\ddagger\,a} = -41 \pm 6$ cal/(mole K)

[a] Errors represent 3σ from a linear least-squares analysis.

termolecular exchange at 120 °C is close to that of 6.4×10^{-5} s^{-1} reported[3] at 130 °C for substitution with PPh_3, both reactions probably proceed by the same CO dissociation mechanism.

Intramolecular exchange occurs at temperatures where the rate of intermolecular CO exchange can be neglected. Rates of intramolecular CO exchange were determined by heating complex III for specific times and then analyzing the label distribution by ^{13}C NMR. Spectral changes for a rate measurement are shown in Figure 2 and the first-order plot of ln $(I_\infty - I_t)$ vs. t for the equatorial CO on Re is shown in Figure 3. Values for rate and activation parameters are given in Table II. Because of signal-to-noise limitations only data for the loss of equatorial ^{13}CO from Re are given. From Figure 2 the rate of loss of the axial ^{13}CO on Re is seen to lag behind that of the equatorial ^{13}CO's. For the best set of spectra (i.e., the 75 °C rate) the rate of loss of the axial CO was ~0.5 that of the equatorial groups. The rate of intramolecular exchange (Table II) also is independent of the complex concentration thereby eliminating bimolecular exchange pathways (e.g., tetranuclear intermediates have been proposed[22] for high-temperature reactions of $MnRe(CO)_{10}$).

Intramolecular CO migration probably occurs by pairwise exchange[23] (e.g., Scheme I), although any species with two or more bridging CO's can lead to exchange. One specific Mn–Re rotamer was selected for the scheme. Similar rearrangements can be drawn for other rotamers; however, we have no information to favor any single choice. Because the intermediate in this mechanism obeys the 18e rule it is somewhat surprising that the exchange process requires a moderately high temperature to proceed. Activation energy data in Table II show that this results not from a large enthalpy of activation but from a large negative entropy of activation. Given the considerable error in observed rate constants the small statistical error in the activation parameters may be fortuitous. Formation of the dibridged structure requires synchronous motion of two *carbonyl* ligands on different metal centers to obtain a structure that satisfies the 18e rule. This could be the origin of the high entropy of activation. Our finding of a high entropic barrier to exchange of all terminal carbonyl groups agrees with the predictions of Band and Muetterties[23] for the pairwise exchange mechanism. The mechanism shown is also expected to exchange axial carbonyls at slower rate ($\sim 0.5k_{eq}$) than the equatorial carbonyls since the axial CO groups must first transfer to an equatorial site before migrating to the other metal center.

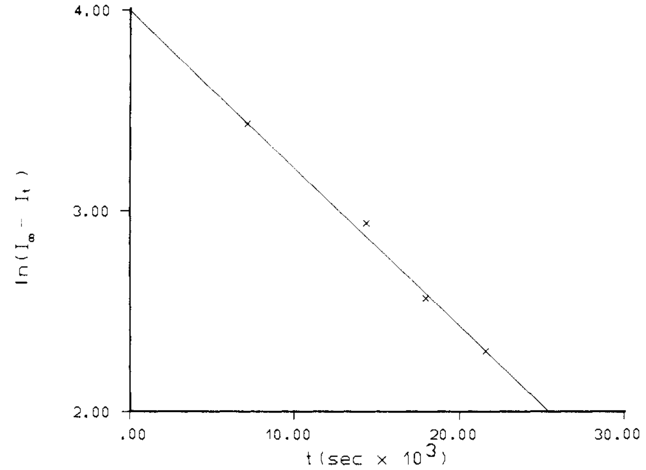

Figure 3. Plot of ln $(I_\infty - I_t)$ vs. t for the intensities of the equatorial carbonyl resonance of Re from the spectra in Figure 2. The line shown is from a linear least-squares analysis.

Scheme I

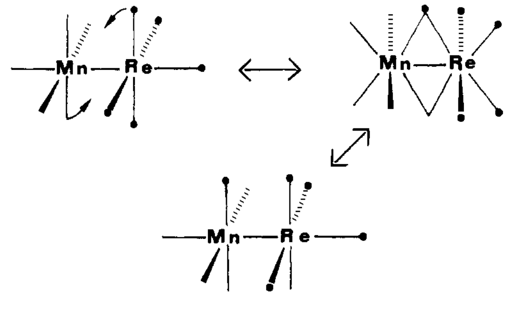

There have been few kinetic studies of CO exchange across nonbridged metal–metal bonds. Exchange of terminal and bridging CO ligands in compounds that contain a bridging CO group in the ground state is common.[24] Adams and Chodosh[25] reported interchange of isonitrile and CO ligands between the two metal atoms of $(CH_3NC)(OC)_4MnMn(CO)_3(CNCH_3)_2$, which contains no bridging ligands. Carbonyl scrambling in $Cp(CO)_3MoMo(CO)_2(CNCH_3)Cp$ has also been shown[26] to proceed by dibridged carbonyl and isonitrile species. Isomerization of 1,2-$Mn_2(CO)_8(CN\text{-}t\text{-}Bu)_2$ to the 1,1 isomer has also been reported.[27] A dibridged intermediate has been proposed[28] for CO exchange in the donor–acceptor complex $(Me_3P)(CO)_5Os \rightarrow W(CO)_5$. Dicobalt octacarbonyl provides an example[29] where bridged and nonbridged isomers exist in equilibrium. A study

---

(22) Marcomini, A.; Poë, A. *J. Am. Chem. Soc.* **1983**, *105*, 6952–6958.
(23) Band, E.; Muetterties, E. L. *Chem. Rev.* **1978**, *78*, 639–658.
(24) Johnson, B. F. G.; Benfield, R. E. In "Transition Metal Clusters"; Johnson, B. F. G., Ed.; Wiley-Interscience: Chichester, 1980.
(25) Adams, R. D.; Chodosh, D. F. *J. Organomet. Chem.* **1975**, *87*, C48–C50.
(26) Adams, R. D.; Brice, M.; Cotton, F. A. *J. Am. Chem. Soc.* **1973**, *95*, 6594–6602.
(27) Robinson, D. J.; Harris, G. W.; Boeyens, J. C. A.; Coville, N. J. *J. Chem. Soc., Chem. Commun.* **1984**, 1307.
(28) Einstein, F. W. B.; Jones, T.; Pomeroy, R. K.; Rushman, P. *J. Am. Chem. Soc.* **1984**, *106*, 2707–2708.
(29) Bor, G.; Noack, K. *J. Organomet. Chem.* **1974**, *64*, 367–372. Sweany, R. L.; Brown, T. L. *Inorg. Chem.* **1977**, *16*, 415–421.

of the interaction between bridging carbonyl ligands and aluminum alkyls has shown[30] that an adduct may form with the bridging carbonyl and AlR_3. An attempt to induce CO bridging in $Mn_2(CO)_{10}$ showed that such an adduct is not formed.[30] Consequently, the dibridged isomer of $Mn_2(CO)_{10}$ does not lie at low energy.

Acknowledgment. This material is based on work supported by the National Science Foundation under Grants No. CHE82-10514 (F.B.) and No. CHE84-02168 (W.C.T.). W.C.T. thanks the Alfred P. Sloan Foundation for a research fellowship. Helpful discussions with Prof. Charles Perrin, Prof. Roald Hoffmann, and Dr. Kevin Stewart are gratefully acknowledged.

---

(30) Alich, A.; Nelson, N. J.; Strope, D.; Shriver, D. F. *Inorg. Chem.* **1972**, *12*, 2976–2983.

A Mössbauer Effect Study of the Electronic Structure of Several Tetranuclear Organoiron Clusters

Christopher G. Benson, Gary J. Long,* John S. Bradley, J. W. Kolis, and D. F. Shriver

Contribution from the Departments of Chemistry, University of Missouri—Rolla, Rolla, Missouri 65401, Northwestern University, Evanston, Illinois 60201, and the Exxon Research and Engineering Company, Annandale, New Jersey 08801. *Received May 20, 1985*

Abstract: The Mössbauer spectra obtained at 78 K for a series of tetranuclear organoiron clusters reveal well-resolved quadrupole doublets with a range of average isomer shifts which may be related to the charge on the cluster. Single-crystal X-ray structural results are available for each of the clusters studied, and the Mössbauer spectra reveal the expected number of crystallographically distinct iron sites. The spectrum obtained for $(PPN)_2[Fe_4(CO)_{13}]$ (I), which contains a tetrahedral iron cluster with a triply-bridged carbonyl on one face, reveals a high electronic symmetry for the unique iron site. The remaining clusters have the butterfly structure and Mössbauer spectra which have clearly resolved doublets for the wingtip and backbone iron sites. The isomer shift values observed for each of the iron sites in several of the butterfly clusters is linearly related to the Slater effective nuclear charge experienced by the iron 4s electrons. The effective nuclear charge has been calculated from the orbital occupation values obtained through Fenske–Hall molecular orbital calculations published by Harris and Bradley. The results indicate that the Mössbauer effect isomer shift, when used in conjunction with detailed molecular orbital calculations, provides an accurate map of the electronic charge density distribution in a cluster. Further it provides insight into how this charge distribution changes with changes in the peripheral ligands in such a cluster.

The role played by surface bound carbon atoms in various metal catalyzed reactions has led to considerable interest in metal cluster chemistry.[1] The spectra of structurally characterized molecular metal clusters provide valuable reference points for the identification of surface species generated in the process of chemisorption and catalysis. Mössbauer effect spectra of organoiron clusters also may aid structural elucidation and provide insight into the electronic environment of the individual iron sites.

The Mössbauer effect spectra of the dianionic bipyramidal iron carbonyl cluster, $(PPN)_2[Fe_4(CO)_{13}]$ (I), and a series of neutral, monoanionic, and dianionic iron carbonyl butterfly clusters, II–VIII, have been measured and do indeed provide important clues to the electronic and structural nature of the clusters. Two previous Mössbauer effect studies of tetrameric iron carbonyl clusters have been reported.[2,3] Some of the present spectra duplicate those which were published earlier, but significantly different results were obtained for others.

Single-crystal X-ray structures are known for all of the compounds in the present study. In all cases, the Mössbauer data are both consistent with and complementary to the single-crystal X-ray structural results.

Experimental Section

All the clusters studied were prepared by using standard literature methods previously reported.[4-9] In all cases the samples were prepared, stored, handled, and measured under a nitrogen atmosphere or under vacuum at 78 K. Mössbauer effect spectra were obtained at 78 K on a conventional Ranger Scientific constant acceleration spectrometer which utilized a room temperature rhodium matrix cobalt-57 source and was calibrated at room temperature with natural abundance α-iron foil. The spectra were fit to Lorentzian line shapes by using standard least-squares computer minimization techniques. The error analysis was carried out by using standard error propagation techniques. In the spectral evaluation, the initial areas used for each iron component in an individual spectrum were based on the number of structurally distinct iron sites obtained from the single-crystal X-ray structure of the relevant cluster. With the exception of $(PPN)_2[Fe_4(CO)_{13}]$ (I), in which the areas of the two components were constrained in the fixed ratio of 3:1, all the components of each spectrum were allowed to vary, either as symmetric or asymmetric doublets, until the best fit was obtained.

Results and Discussion

The Mössbauer effect spectra were fit to quadrupole split doublets of independent areas and are shown in Figures 1 and 2. The resulting Mössbauer spectral parameters are listed in Table I. The value of $\sum\delta$ included in this table is the sum of the isomer shifts for each iron site in the cluster. The spectral fits are good, as indicated by the low χ^2 values and the goodness of fit illustrated in the figures. Under these conditions, the value of $\sum\delta$ is independent of spectral assignment. The value of $\Delta\delta$ is the shift in the isomer shift for a particular iron site in the cluster relative

---

(1) Muetterties, E. L.; Rhodin, T. N.; Band, E.; Brucker, C. F.; Pretzer, W. R. *Chem. Rev.* **1979**, *79*, 91–137.

(2) Farmery, K.; Kilner, M.; Greatrex, R.; Greenwood, N. N. *J. Chem. Soc. (A)* **1969**, 2339–2345.

(3) Sosinsky, B. A.; Norem, N.; Shelly, J. *Inorg. Chem.* **1982**, *21*, 348–356.

(4) Edgell, W. F.; Yang, M. T.; Bulkin, B. J.; Bayer, R.; Koizumi, N. *J. Am. Chem. Soc.* **1965**, *87*, 3080–3088.

(5) Tachikawa, M.,; Muetterties, E. L. *J. Am. Soc.* **1980**, *102*, 4541–4542.

(6) Holt, E. M.; Whitmire, K. H.; Shriver, D. F. *J. Organomet. Chem.* **1981**, *213*, 125–137.

(7) Manassero, M.; Sansoni, M.; Longoni, G. *J. Chem. Soc., Chem. Commun.* **1976**, 919–920.

(8) Bradley, J. S.; Ansell, G. B.; Hill, E. W. *J. Am. Chem. Soc.* **1979**, *101*, 7417–7419.

(9) Bradley, J. S.; Ansell, G. B.; Leonowicz, M. E.; Hill, E. W. *J. Am. Chem. Soc.* **1981**, *103*, 4968–4970.

0002-7863/86/1508-1898$01.50/0